Detection of non-ionising radiation by its effect on the parameters of TADF (thermally activated delayed fluorescence) and its application in observing celestial objects

ABSTRACT

A new method is proposed for detecting non-ionising radiation, based on measuring parameters of TADF (thermally activated delayed fluorescence) that occurs in an excited luminophore. We present the advantages of this method, which include high sensitivity, small size and low cost of the apparatus, as well as providing the ability to perform observations even when there are obstacles in the direct line of sight. We show that celestial objects can be detected using this apparatus, demonstrating that such objects are a robust source of non-ionising radiation. Readings and result sets collected over time from different detectors placed in different parts of the Earth show consistency with each other. There is also consistency of results of a single detector taken over several days, proving that the method and the apparatus used are reliable for observing celestial objects.

IONISING AND NON-IONISING RADIATION

Ionising radiation consists of waves and/or particles with enough energy to knock out electrons from atoms or molecules. This may result in altering the medium in which this radiation is travelling, either by direct destruction of the molecules or by promoting reactions with the newly formed radicals. Non-ionising radiation, which will also be composed of particles and/or waves, possesses no such large amounts of energy but can still affect the medium in which it is travelling by modifying some of the parameters of dynamic processes, influencing rates of reaction, probability distributions etc. These differences also determine how each type of radiation is detected. Ionising radiation is mainly detected by the ionic products of the penetration of ionising radiation into the medium. Non-ionising radiation is detected by its influence on observed processes.

Processes that are appropriate for observation are such that on a macroscopic scale appear to be continuous functions with respect to external factors, for example temperature, pressure, resistance etc. For individual atoms or molecules, the functional dependence could be discontinuous, but statistically the dependence appears to be continuous because phase transitions do not take place simultaneously in the whole medium. Consequently, there is statistically a number of events large enough to be detected. This allows for high sensitivity of detection, since even the smallest change in an external factor can induce a corresponding change in an observed physical process.

The method that we propose for detecting non-ionising radiation involves the use of a luminophore that exhibits TADF. The intensity I of the emitted by the luminophore radiation obeys the Arrhenius equation

$$I = Ae^{-k/T}$$

where A and k are constants and T is the absolute temperature, and therefore falls into the category of continuous processes appropriate for detecting non-ionising radiation with high sensitivity.

BASIC PRINCIPLES OF TADF

TADF (Thermally Activated Delayed Fluorescence) occurs because of the close proximity of energy levels S_1 and T_1, to which electrons can be excited from the ground level by visible light from an LED. The TADF material and the LED are chosen so that the photon energy from the LED is no less than the energy difference between the ground singlet state S_0 and the triplet state T_1 in the material. The reverse

transition is generally prohibited by quantum mechanical rules and therefore occurs at a relatively slow rate within a time interval of the order of 1 μs. Such a transition is usually called phosphorescence.

According to Stokes rule, the wavelength at maximum intensity of the emission spectrum during photoluminescence is larger than the corresponding wavelength of the absorption spectrum. Since photon energy is inversely proportional to the wavelength, $E = hc/\lambda$, the minimum excitation energy must be higher than a particular minimum value. On the other hand, if the excitation energy is higher that the difference $T_1 - S_0$, then according to Kasha's rule any electron that is excited to the levels S_i, T_i, (i > 1) will undergo a transition to the levels S_1 and T_1 over a short time interval by internal conversion (IC), meaning that the excess energy will be mostly transferred to heat. Photon emission will only take place when electrons move to the fundamental level S_0 either from the triplet level T_1 (phosphorescence), or from the singlet level S_1 (fluorescence).

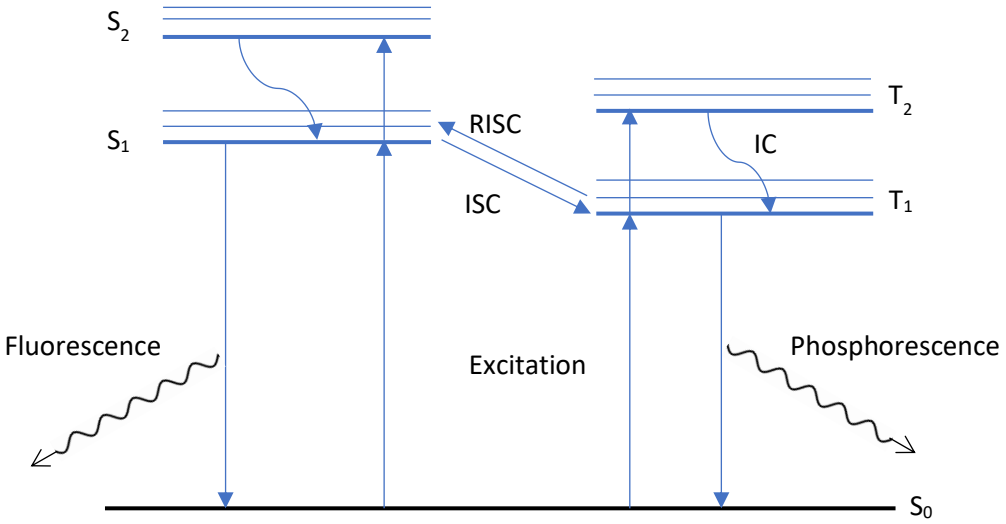

Pic. 1

The singlet-singlet transition, $S_1 \rightarrow S_0$, usually called fluorescence, is a process much faster than phosphorescence, occurring usually over a time interval of the order of 10 ns. The delay, highlighted in the name of the process, is due to reverse intersystem crossing (RISC), in which electrons absorb surrounding thermal energy to manage the transition $T_1 \rightarrow S_1$, followed by a fast transition to the fundamental level S_0. How fast the RISC transition will take place depends on the energy difference between the singlet S_1 and triplet T_1 energy levels: the smaller the energy difference, the faster the RISC transition will occur. The direct transition $S_1 \rightarrow T_1$ (ISC) is also possible.
The corresponding energy and levels and sublevels, as well as the possible transitions, are schematically shown in Pic. 1.

We should note the significance of thermal fluctuations in the TADF process. The energy difference between the ground state S_0 and first excited states S_1 and T_1 is too large for these fluctuations to excite an electron to these energy levels, so the excitation of the luminophore is achieved by the use of an excitation source, for example an LED. On the other hand, the energy difference between the first excited states themselves, considering also their sublevels, is much smaller and so the transitions between them can take place due to thermal fluctuations. These may include transitions in which electron energy is increased, like RISC, or decreased, like IC, but in all of these transitions, there is no photon emission or absorption involved. In the excited luminophore there will always be electrons at an energy level infinitesimally close to S_1. The transition to S_0, on the other hand, cannot be implemented without a photon emission. These circumstances lead to Kasha's rule. Since any excited electron can potentially cause TADF emission, then the number of electrons with energy $\mathrm{E} \geq S_1$ is proportional to the intensity of the TADF emission.

The energy fluctuations of the electrons may be evoked also by other factors and by radiation. Once the level of thermal fluctuations is fixed or measured, any deviation in the TADF emission will be attributed to other factors, including external radiation. The main concept of detection depends on the availability of large numbers of photons so that the use of statistical considerations is valid. The device captures individual photons of more or less the same energy and there must be a sufficient intensity of such photons (number of photons per unit time per unit area) for them to be registered as a distinct signal. Therefore, the processes that can be detected are such that provide a sufficient number of electrons with energies above a minimum threshold value. Thermal fluctuations obviously fulfil these conditions, but so do other factors. The sensitivity of this method in detecting external radiation is quite high since the energy difference between close sublevels, which electrons can be excited to, is extremely low: in the excited state the luminophore always contains a large enough number of electrons with energies $E > S_1 - \Delta$, where Δ is an infinitesimally small number.

Specifically, this condition is the one that accounts for the high sensitivity of the method in use. Small amounts of energy will, directly or indirectly cause the gradual ascension of electrons up the energy scale, to the point where they will spontaneously descend to S_0 emitting a photon. So keeping the luminophore in an excited state with an appropriately adequate number of electrons is critical for detecting low energy level radiation.

Energy fluctuations of electrons may be caused by a wide range of external radiation types; therefore, the device should be shielded from undesirable radiation, or their influence should be excluded either by specialised construction techniques and/or by being taken into consideration during measurements.

The experimental assembly is based on a sensitive element (a luminophore exhibiting TADF) excited by an LED. The arising luminescence is registered by a photodiode. Special construction elements are used in order to minimise the effect of undesirable factors during the process of measuring the TADF intensity.

RADIATION ON THE EARTH'S SURFACE

Earth's atmosphere will absorb most of the ionising electromagnetic radiation from the Sun. Barely any radiation with a wavelength of less than 200 nm reaches the surface of the Earth [4]. This means that gamma and X-rays do not penetrate the atmosphere. The remaining ionising part UVC, can be excluded with a shiny metal surface.

The Sun also ejects a large number of charged and uncharged particles. This is true for all other stars, galaxies and so forth, that can additionally be the source of very energetic and very penetrating gamma rays. Therefore, the list of particles reaching the Earth from outer space includes all subatomic particles and their antiparticles, heavier leptons and antileptons, various hadrons as well as heavier nuclei and antinuclei [5]. A large number of these is caught and diverted by the magnetic field. Those that do enter the atmosphere will rarely reach the surface due to high ionising ability but are energetic enough to cause a cascade of secondary ionisations that eventually reach sea level. These secondary ionisations may also result in the production of mesons, muons and antimuons. Muons and antimuons have also been detected under water.

Charged particles have a high interaction cross section and can therefore impart large amounts of energy to the system (luminophore molecule). So appropriate shielding should be used if ionising radiation is to be excluded in the observations. Conversely, neutral particles have a very small interaction cross section. Neutrons will primarily engage in strong interactions, which excludes significant interaction with leptons like electrons. Neutrinos have an even smaller interaction cross section with other particles. Uncharged particles cannot be shielded out, but should rather be considered as part of the non-ionising radiation responsible for the TADF effect on the luminophore.

DISCRETE SENSOR

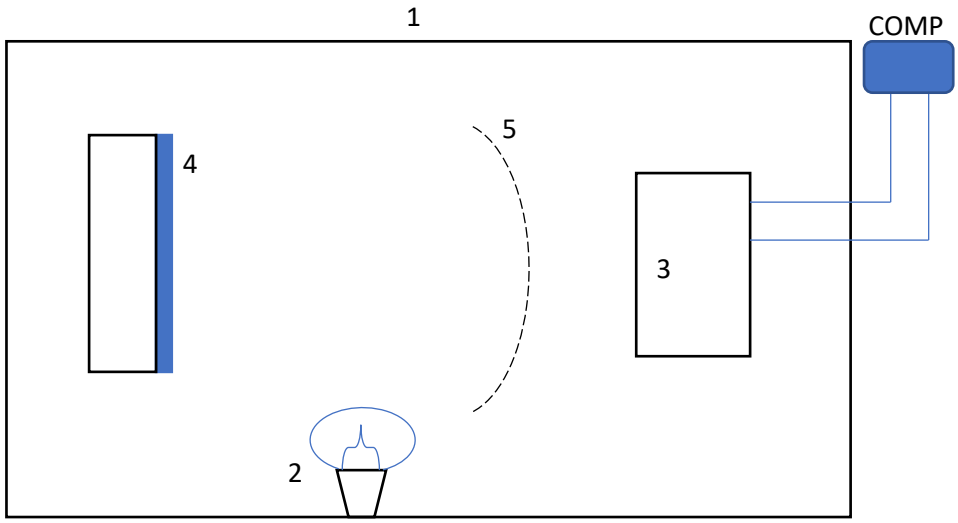

Pic. 2

The main components of the device are the following:

1 Housing for shielding from ionising and other undesirable external radiation.
2 One or more LEDs as radiation sources for the excitation of the luminophore.
3 A detector of TADF emissions. Any known type of photodetectors may be used, as long as it is sufficiently sensitive in the TADF frequency range of the luminophore being used. The output signal from the detector is amplified and filtered by electronic circuitry, then digitised and passed on to a microprocessor for further manipulation.
4 Luminophore with TADF properties.
5 An optical filter (optional) placed between the luminophore and the emission detector to single out the TADF emission and suppress other types of emission (e. g. phosphorescence) if they are emitted simultaneously but differ in frequency.

The shielding housing

Critical for excluding ionising radiation with the use of thick metallic casing.

The luminophore

Basically, any material that demonstrates TADF properties may be used as a luminophore. The material used in our experiment was a mixture of fluorescein natrium and boric acid in the ratio of 1:10000, that had undergone partial dehydration by heating to a temperature of 200 C. As mentioned earlier, the material used obeyed the Arrhenius equation and was therefore able to exhibit high sensitivity due to a continuous dependence of intensity on temperature.

The TADF detector

Various types of photodetectors may be used as a TADF detector. In our experiments, we made use of discrete silicon CCD photodiodes.

DISCRETE SENSOR in detail

The basic principles of operation of a discrete sensor are illustrated in Pic. 3 where the main blocks and connections are presented in a simplified form.

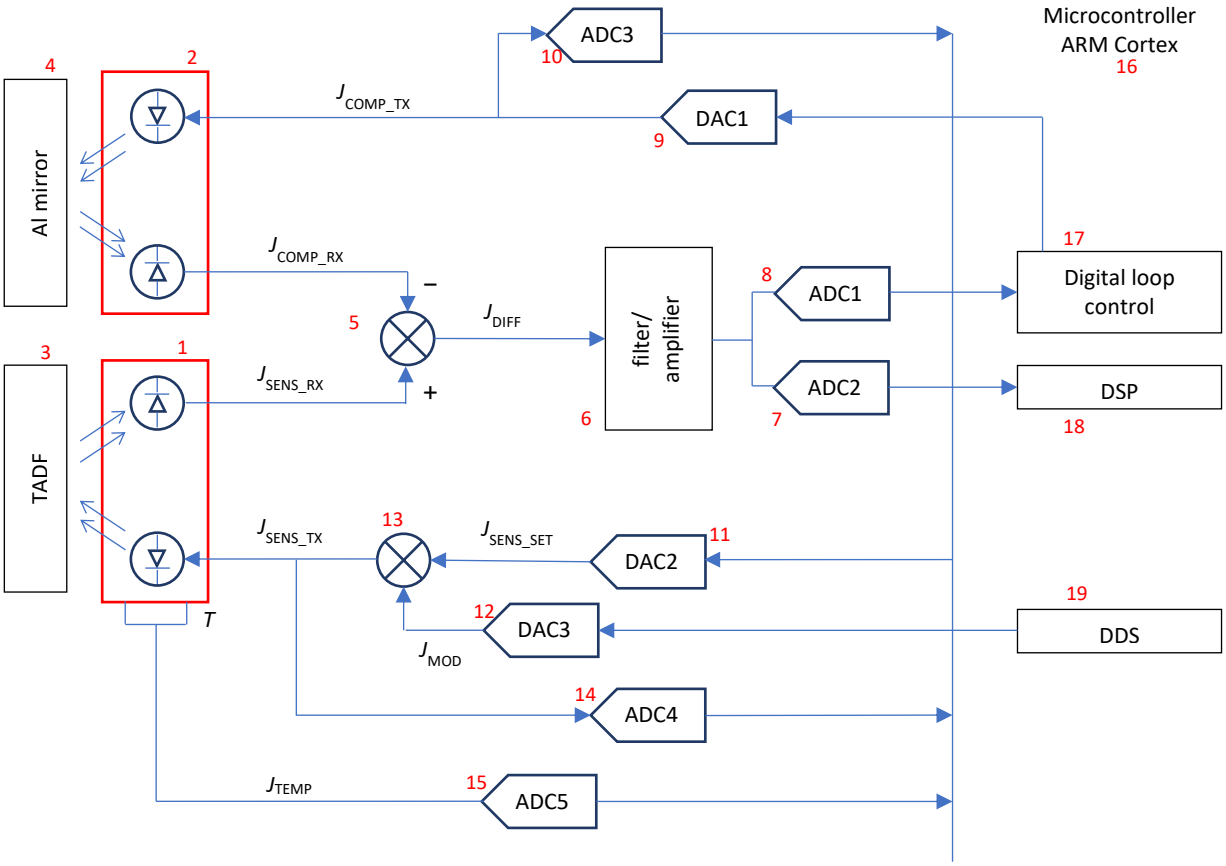

Pic. 3

The sensor contains two identical photodiode + LED assemblies. Assembly (1) is coupled with a TADF material (3) and carrying out the main measurements. Assembly (2) is set next to a non-transparent aluminium mirror (4) and is used as a compensating set. The primary photocurrent J_{SENS_RX} from assembly (1) and the secondary photocurrent J_{COMP_RX} from the compensating assembly (2) are fed to the adder, where J_{COMP_RX} is subtracted from J_{SENS_RX}. The difference current J_{DIFF} is fed to the filter/amplifier (6), which is a multistage circuit consisting of linear analogue elements. The output from (6) goes to a fast feedback loop ADC1 (8) and a measuring ADC2 (7).
The output signal from ADC1 is used by the compensation digital loop control (17), which is part of the microcontroller (16), which in turn goes to DAC1 and the resulting current J_{COMP_TX} is fed to the LED of the compensating assembly (2).
The output from ADC2 is fed to the DSP (18) which is also part of the microcontroller (16). There it undergoes processing, including filtration and compensation for interfering factors like temperature variations of the luminophore, various parameters of the surrounding medium, assembly excitation currents, supply voltages etc.
The operating current J_{SENS_SET} (a profile of the excitation current) is set by the microcontroller (16) software. Passing through DAC2 (11) and an adder (13) the excitation current is fed to the LED of the measuring assembly (1). The second input to the adder (13) consists of the modulation current J_{MOD} formed by the microcontroller (16) and transformed to an analogue form by DAC3 (12). If harmonic modulation is used, then the signal is formed by the frequency synthesizer DDS (19), the software for which is also part of the microcontroller software.

The assembly excitation currents J_{SENS_TX} и J_{COMP_TX} are digitised by ADC3 (10) and ADC4 (14) and fed to the microcontroller (16). The microcontroller also receives data about the luminophore temperature, which is measured by a sensor mounted directly on the luminophore and then digitised by ADC5 (15).
Such circuitry makes it possible to operate the sensor in any excitation mode (constant mode, impulse mode, periodic mode, or even by a signal of arbitrary form). In practice, the resolution capacity of the circuitry enables it to record intensity variations corresponding to the emission of one photon in 2 seconds. The use of the compensating assembly makes it possible to eliminate the influence of most external factors (including ionising radiation) at the photodetector itself. Measuring and taking into account algorithmically significant sources of deviation and disturbances, as well as shielding from external electromagnetic radiation, enables a reliable measurement of non-ionising radiation as such.

Several types of discrete sensors were constructed, varying from one another in the implementation of the measuring and compensating assemblies. Data sets received from each of these sensors correlate well with each other, with solar monitoring data, as well as some astronomical events. As a result, the following hypothesis was formulated, that astronomical objects would act as sources of the detected non-ionising radiation.

SHIELDING

The shielding of the detector is critical for excluding influence from ionising radiation. The sensitive element of the detector is placed under a solid steel screen covered with lead, while the detector itself is in a hermetically closed case providing a seal from external humidity and other factors. The power supply of the detector passes through two consecutive galvanic barriers with multi-stage filters, which isolate the signal from possible noise interference. Nevertheless, various parameters are constantly being recorded: fluctuations of voltage supply, excitement currents for the measuring and the compensating channels, temperature of the sensitive element and of the detector, pressure and humidity inside the casing, as well as mechanical vibrations and electromagnetic perturbations inside the detector using a magnetometer and an accelerometer. Finally, the compensating circuit makes it possible to single out those phenomena in the measured signal that are exclusively associated with fluctuations in the brightness of the luminophore, since all other factors affect both channels in identical ways.

Such measures allow the control, or even exclusion, of the effect of fluctuations of external physical factors as well as external ionising and electromagnetic radiation. The circuitry used makes it possible to suppress a large proportion of external interfering components even at the stage of detection and registration of the signal. The rest is dealt with by using an appropriate algorithm. Parameters that could potentially interfere with our measurements include temperature, pressure, humidity, as well as interference from the power supply and industrial or domestic electromagnetic sources. Using such precautions as described, we achieved lack of correlation of fluctuations of these parameters with the readings of our detectors in the frequency range of interest. These results have been verified upon exposure to external electromagnetic waves in the frequency range of 10 Hz – 3 GHz.

Consequently, the types of radiation that can presumably influence the detecting device are:
- weakly interacting neutral particles (fast neutrons, neutrinos),
- weakly interacting massive particles (WIMP),
- deep penetrating particles and waves (cosmic and nuclear radiation).

Twenty identical discrete detectors were built that have been placed at different parts of the Earth including Moscow, Riga, Paphos (Cyprus) and Rome. The recorded data is collected on servers and analysed. The analysis shows that data from different detectors is consistent and correlate well, proving celestial objects to be good sources of detectable non-ionising radiation. These detectors are shown in Pic. 4.

Pic. 4
Discrete detectors with casing and connections used in our experiments.

DIRECTIONAL MATRIX SENSOR

Based on the hypothesis that astronomical objects could be the sources of the detectable modulated TADF, as well as the assumption that the external radiation could influence the isotropy of TADF emissions, a directional matrix sensor was developed for determining the direction and intensity of the source of non-ionising radiation.

The matrix sensor was developed as an attachment to a digital camera that was itself placed on an azimuth mount. The attachment consisted of a luminophore plate and a circuitry for exciting (illuminating) the luminophore, as well as accessory sensors (for measuring temperature, pressure, electromagnetic field intensities). During operation the camera was functioning at the same time as the illumination circuitry and provided measurements of the luminophore emissions a specified time after the illumination was turned off. The camera was producing images at a rate of 100 Hz. The processing of all data output from a matrix sensor was done by a specialised software. The availability of literally thousands of parallel channels made it possible to effectively filter out possible interfering effects (the images of which always appeared out of focus, unlike those of the useful signal).

The camera with the matrix sensor was set up on an azimuth mount and placed in a room with concrete walls and ceiling. The sensor element of the detector (in the form of a camera attachment) was isolated in a selected specified direction by a multilayer screen consisting of micarta, copper, aluminium, glass and polymer gaskets with a total thickness of 4 cm. The components of the matrix sensor are shown in Pic. 5.

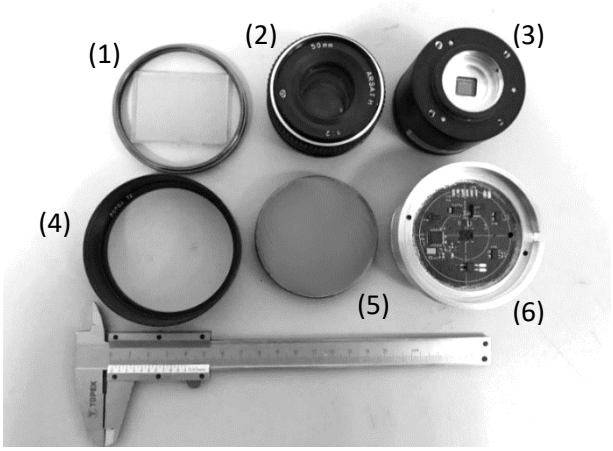

(1) Sensor element of the detector (luminophore plate)
(2) objective lens
(3) digital CCD camera
(4) attachment with a polarising filter
(5) aluminium screen
(6) excitation circuitry

Pic. 5

DESCRIPTION OF THE EXPERIMENT

The sensor was directed to the south with the intention that in the course of the daily rotation of the Earth the detector would scan a strip of the sky around 10 degrees in width near the celestial equator (Pic. 6).

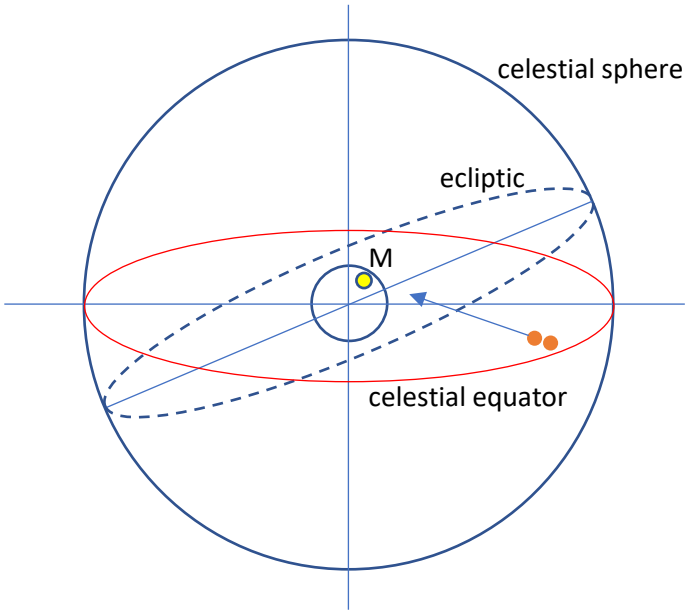

Pic. 6

Pic. 7 shows an example of the kind of images obtained by the sensor. In the course of our main experiment a matrix sensor remained motionless and was operating continuously for 17 days, providing 17 scans of the same strip along the celestial equator. We collected approximately 6 TByte of data and required around 6 months to process them. A spectral analysis was performed for every observable point in space to construct a spectral portrait of that object for every day of the experiment. We then compared the relative portraits for a single dot over the 17 days and identified narrow-band spectral components, characteristic narrow frequency maxima that were apparent in each of the 17 scans.

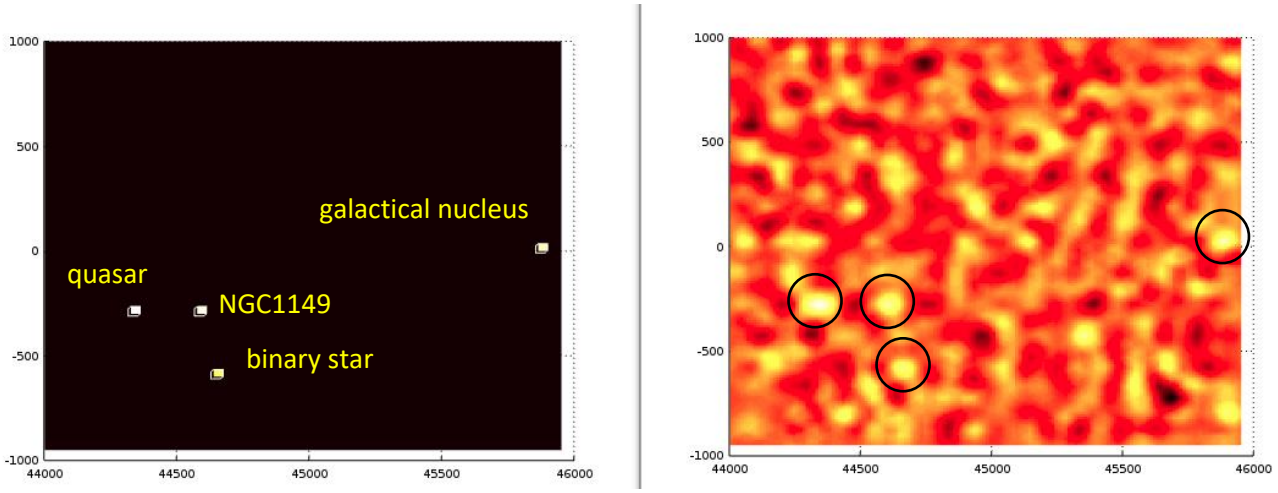

Рис. 7

The image on the right shows a section of the sky in terms of the intensity of the detected radiation. The x-axis and y-axis show RA and DEC angles respectively in centidegrees.

The image on the left shows the 4 strongest signals. The strongest of them belongs to the second left dot and corresponds to galaxy NGC1149.The other 3 maxima belong to a quasar (SDSS J025641.83-002353.7), a binary star (HIP13766) and a galactical nucleus (SDSS J030243.6-000608).

The frequency of registered signals may vary from one scan to the next if the source of the signal is in motion, rotational or otherwise. Yet we were able to identify such signal sources the spectrum of which contained highly stable harmonic components. Pic. 8 shows the spectrogram from the signal of one such source, supposedly incorporated in galaxy NGC6964. The horizontal axis represents frequency in mHz, the vertical axis represents the day of observation (1 through 17 of the experiment). Bright dots on dark background are spectral maxima. The bright vertical line is a distinct monochromatic signal of frequency 18.059 Hz.

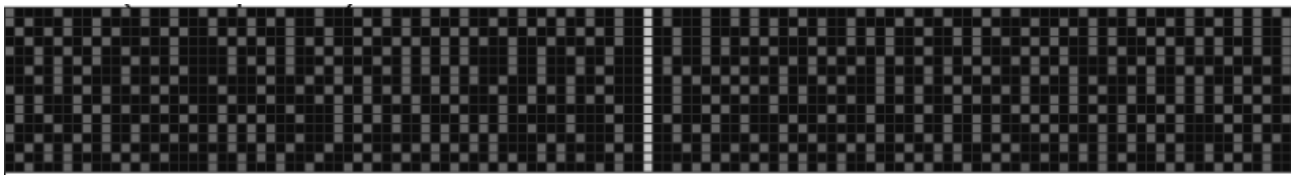

Pic. 8

In our observed sky strip, we were able to identify many dots that had such distinct components in their spectrum. Approximately 90% of them can be matched to a visible object since at least one star is present in the immediate coordinate vicinity of every such dot. Of course, this is expectable, considering the intense activity of modern astronomy.

The decisive image was the one obtained of the galactic pair NGC1143-NGC1144, which turned up in our strip of observation. The image is presented in Pic. 9a, and for comparison in Pic. 9b the IR image of the same pair is given [6]. We can see that the signal intensity is high enough for the matrix sensor to capture even the galactic halo. The coordinates recorded by the matrix sensor and the IR telescope coincide within an uncertainty of less than 0.5°, which is in agreement with the systematic error of the sensor installation.

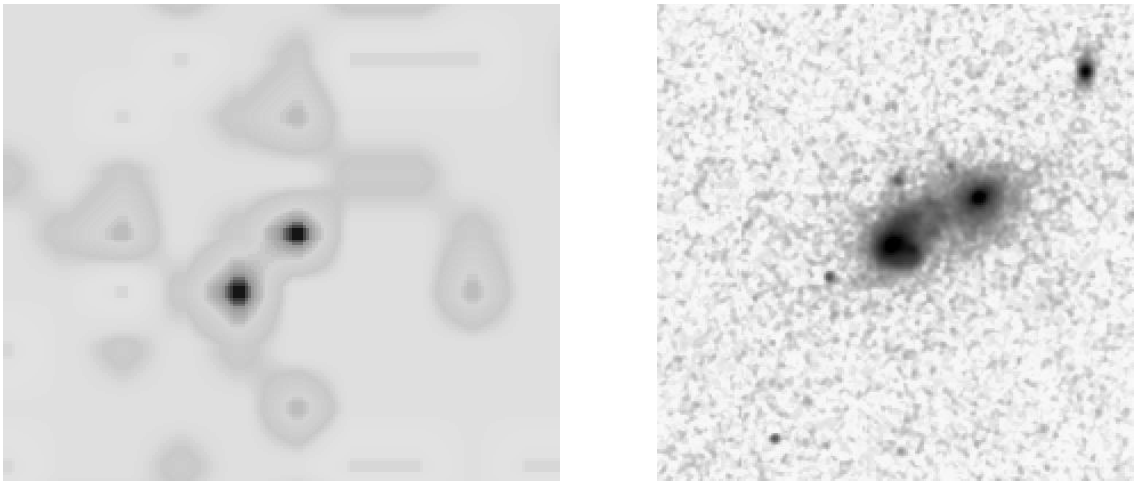

a
With the use of the matrix sensor

b
In the IR range

Pic. 9

The analysis of the gathered results shows that they are consistent over the 17 days proving they are in good correlation.

CORRELATION OF MEASUREMENTS

To ensure that the detectors react indeed to external signals from space, data from two different discrete detectors was gathered and checked for correlation. One detector was positioned in Italy, the second detector in Cyprus. The distance between the two detectors was 2200 km. The difference between the longitudes of these points is 21.91°. The difference between the latitudes is 10.91°.

The output signal of each discrete detector was first subjected to bandpass filtering using high and low frequency EMA first order filters, retaining the frequencies in the 0.003 – 25 Hz band. The detectors were placed on horizontal surfaces in buildings made of stone, in temperature-controlled rooms. The thermal time constant of the detectors housing is 2520 sec.

The Earth rotates at an angular speed of 15° per hour, or 1° every 4 minutes. This means that the longitude difference between the two points where detectors are positioned corresponds to a time interval of 87.5 minutes. That should be the delay time between detections made by the two sensors as they align with the external signal source due to the Earth's rotation. The graph of the cross-correlation function between the two detectors is given in Pic. 10. The relative value of the cross-correlation function

$$F_{12}(\tau) = (f_1 * f_2)(\tau)$$

is plotted on the y-axis against time on the x-axis. The graph peaks at 87 minutes with a period of 24 hours, showing clearly consistent sensor reaction to external space signals. The next diagram, Pic. 11, shows the same graph but in greater detail zooming in at the vicinity of one of the maximum points to clearly portray the correlation peak around the 87-minute mark.

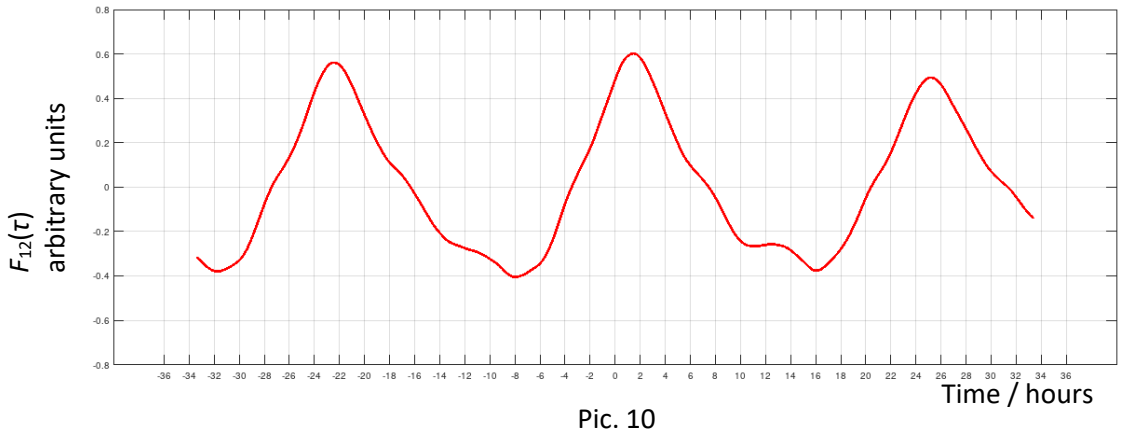

Pic. 10

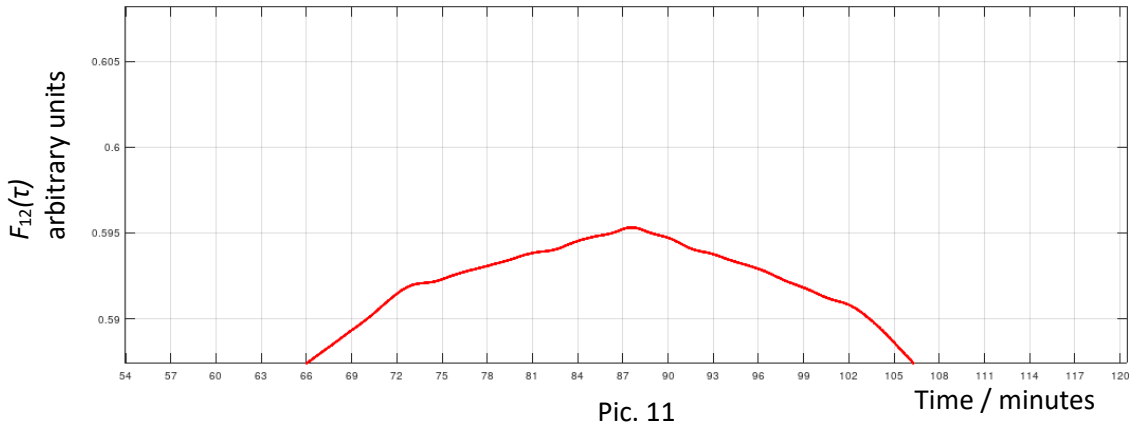

Pic. 11

To study the extent of consistency of data gathered from a single detector a self-correlation function

$$F(\tau) = (f * f)(\tau)$$

was also constructed based on the output signal of a single discrete sensor. The result is shown in Pic. 12. It is clearly evident that the function has a period of approximately 24 hours. The graph in Pic. 13 zooms in again at one of the side maximum points. It shows that the maximum is actually less than 24 hours. It is in fact 23.95 hours (23 hours 57 minutes), the period is closer to the duration of the stellar day, which constitutes 23 hours 56 minutes 4 seconds or 23.934 hours. The percentage error is 0.06% can be attributed to the fact that a relatively wide frequency band is being processed, that can be influenced by processes on the Sun and the Moon.

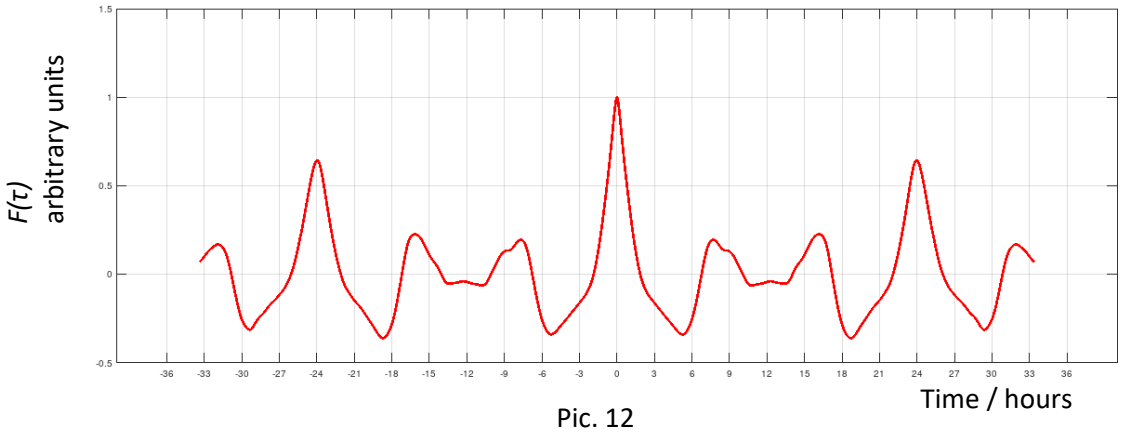

Pic. 12

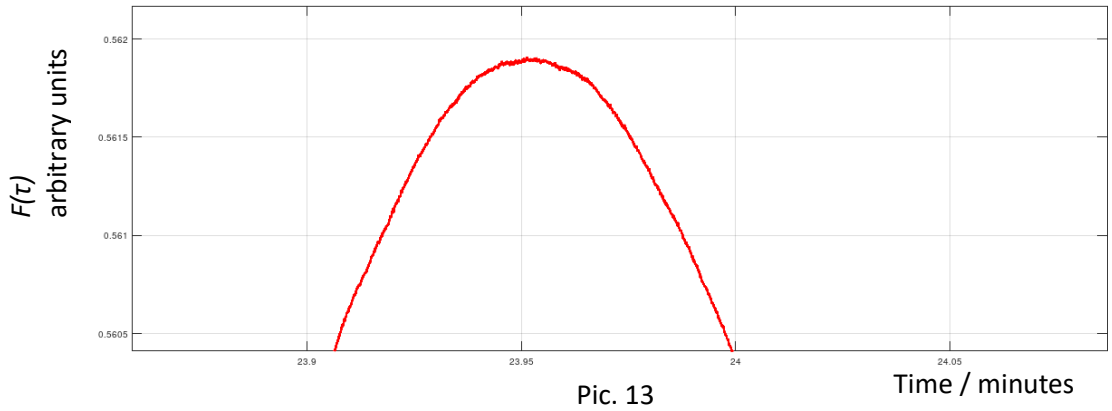

Pic. 13

The final correlation was performed to determine the suitability of the sensor to detect and monitor an external signal of a specific frequency that could be used as a prototype for the navigational system. The system singles out a given frequency by performing a high resolution PLL algorithm. The frequency to be monitored was chosen to be 59.894 Hz, double the rotational frequency of the Crab Pulsar. The outcome is shown in Pic. 14. The blue line depicts the theoretical change of impulse frequency due to the Doppler effect resulting from the daily rotation of the observation point together with the Earth. The red line is the actual change in frequency measured by the detector. The measurement averaging time was 1.5 hours. No amplitude or phase shift normalizations were carried out, these are raw results received directly from the device showing the extent to which amplitude and phase shift values are close to the theoretical ones.

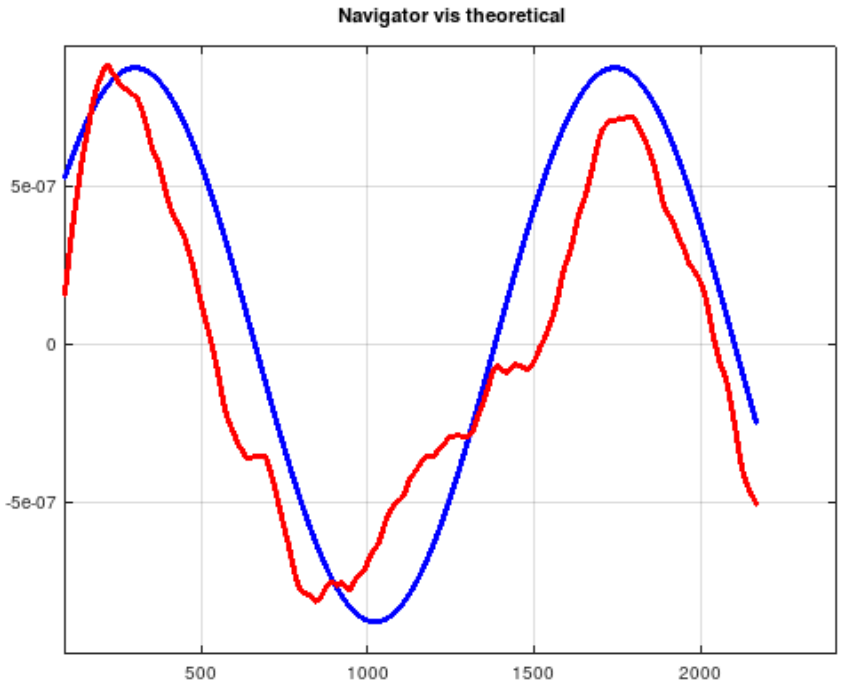

Pic. 14

Following this, we can confidently indicate the existence in space of concentrated powerful sources of non-ionising radiation, as well as the ability of our sensors to detect and record it.

CONCLUSION

The proposed method of detecting non-ionising radiation by its impact on the parameters of TADF has been experimentally confirmed.
The described method shows consistency of data collected at different times and different places from the surface of the Earth
Therefore, we hold that it can be used as a framework to build sensors of non-ionising radiation that enable the determination of the intensity, as well as the direction of propagation of the non-ionising radiation.

In accordance with the principles described in this paper, we have developed prototypes of discrete and directional matrix detectors, and we have patented the method, described in this paper, of detecting non-ionising radiation [7], as well as a method for creating a navigational system, operating on signals of natural sources of non-ionising radiation found in space [8]. Similar methods of using pulsars for autonomous navigation in space have been in development for some time now. They are based on identifying a number of millisecond X-ray pulsars by their emitted signals and consequently calculating the relative position of a spacecraft. Errors in this method are dominated by the inaccuracy of the pulse profiles templates and are estimated by Becker et al. at ±5 km in the solar system and beyond [9]. In this sense, our sensors can be used as an effective means to detect and identify pulsars by the non-ionising radiation that they emit. The signals that our sensors register, independent of their nature, are more consistent than the modulated X-ray emissions of pulsars and consequently result in smaller error during phase measurements. This in turn is expected to lead to significantly smaller navigational errors. Indeed, in some of our experiments we managed to achieve a dispersion in the phase measurements that amounts to an error of just 1 m in calculating the corresponding change in distance.

REFERENCES

1. *Experimental Methods in Chemical Kinetics. Tutorial. Luminescence*
   Red. by: N.M. Emanuel, M.G. Kuzmin, Moscow, MSU, 1985 (in Russian)
   http://www.chemnet.ru/rus/teaching/kinetics-exp/lumene/
2. Eng, J., Penfold, T.J.
   Open questions on the photophysics of thermally activated delayed fluorescence.
   Commun Chem **4,** 91 (2021).
   https://doi.org/10.1038/s42004-021-00533-y
3. Hajime Nakanotani, Youichi Tsuchiya, Chihaya Adachi
   Thermally Activated Delayed Fluorescence for Light-emitting Devices
   Chem. Lett. 2021, 50, 938–948.
   https://doi.org/10.1246/cl.200915
4. Lucien Wald
   Basics in Solar Radiation at Earth Surface
   HAL Archives ouvertes, 2018
   https://hal-mines-paristech.archives-ouvertes.fr/hal-01676634/document
5. Peter Grieder
   Cosmic Rays at Earth. Researcher's Reference Manual and Data Book
   2001, ISBN 0444507108
   http://theor.jinr.ru/~vnaumov/Eng/JINR_Lectures/books/Grieder2001.pdf
6. NASA/IPAC Infrared Science Archive
   https://irsa.ipac.caltech.edu/cgi-bin/2MASS/LGA/nph-lga?objstr=ngc1144
7. US patent 10,794,926
   https://www.freepatentsonline.com/10794926.html
8. US. Pat 10,908,289
   https://uspto.report/patent/grant/10,908,289
9. W. Becker, M.G. Bernhardt, A. Jessner
   Interplanetary GPS using pulsar signals
   Astron.Nachr. /AN 336, No.8/9, 749 ‐ 761 (2015)
   https://doi.org/10.1002/asna.201512251